ELSEVIER

Nuclear Instruments and Methods in Physics Research A 412 (1998) 238–246

NUCLEAR INSTRUMENTS & METHODS IN PHYSICS RESEARCH Section A

Charge collection efficiency in heavily irradiated silicon diodes

L. Beattie, T.J. Brodbeck, A. Chilingarov*, G. Hughes, P. Ratoff, T. Sloan

Department of Physics, Lancaster University, School of Physics and Chemistry, Lancaster LA1 4YB, UK

Received 14 January 1998; accepted 11 March 1998

Abstract

The Charge Collection Efficiency (CCE) has been measured for minimum ionizing particles and for α-particle illuminations from both sides for planar diodes irradiated by neutrons and pions with fluences up to $3 \times 10^{14}\,cm^{-2}$. Geometrical effects on the CCE for partially depleted detectors are deduced from the data as well as trapping effects for electrons and holes.

PACS: 07.77. – n; 85.30. – z

Keywords: Irradiated silicon detectors; Charge collection efficiency

1. Introduction

The present study was performed as a part of the R&D work for the Semiconductor Tracker (SCT) which is a component of the ATLAS experiment [1] at the LHC. It extends the information about the Charge Collection Efficiency (CCE) in irradiated Si detectors [2–4] to fluences well above $10^{14}\,n/cm^2$. In addition to the depletion voltage the CCE is one of the most important parameters determining the operation of SCT after heavy irradiation. The possibility to operate detectors very close to or even below the full depletion voltage also depends crucially on the CCE under such conditions.

The diodes described in this paper are the test structures (kindly provided by the Liverpool University ATLAS group) produced by Micron Semiconductors together with strip detectors of various designs [5]. The diodes therefore can be regarded as typical in terms of the technology and materials used recently for microstrip detectors. All the diodes were made from n-type Si. They have a sensitive area of $5 \times 5\,mm^2$ surrounded by a guard ring and a thickness of $\sim 300\,\mu m$. Before irradiation their depletion voltages were between 10 and 30 V.

The diodes were irradiated at two places: at ISIS (RAL) by neutrons with energy ~ 1 MeV and at PSI (Villigen) by 300 MeV/c pions. The range of fluences used is $(1–3)10^{14}\,cm^{-2}$. All the irradiations were performed at room temperature and without bias. The fluence values for pions are used directly while those for neutrons are corrected to the equivalent fluences of 1 MeV monoenergetic neutrons

*Corresponding author. Tel.: +44 1524 594627; fax: +44 1524 844037; e-mail: chilinga@lavhep.lancs.ac.uk.

0168-9002/98/$19.00
PII: S0168-9002(98)00469-0

Table 1
Diode and irradiation details

Diode no.	Irrad. type	Fluence 10^{14}(cm^{-2})	Thickness (μm)	Initial $U_{dep}(V)$	Irrad. time(d)	Anneal. time(d)	Final $U_{dep}(V)$
4	Pion	1.15 ± 0.07	304	10.2	2	6.5	179
14	Pion	1.26 ± 0.07	300	12.7	2	6.5	209
32	Pion	2.50 ± 0.09	301	12.5	4	4.5	313
28	Pion	2.65 ± 0.08	294	13.4	4	3.5	309
9	Neutron	1.07 ± 0.08	297	15.0	1.8	8.0	161
41	Neutron	1.07 ± 0.08	303	33.5	1.8	7.0	143
7	Neutron	1.32 ± 0.11	296	14.5	3.2	5.0	268
42	Neutron	1.32 ± 0.11	298	33.6	3.2	4.0	211
13	Neutron	2.14 ± 0.10	303	12.9	4.2	5.0	347
49	Neutron	2.14 ± 0.10	307	14.5	4.2	2.0	319
46	Neutron	2.75 ± 0.18	314	14.6	5.0	2.0	386

using hardness factor 1.1 taken from Ref. [6]. After the irradiation the diodes were kept at room temperature for several days until their depletion voltage ceased to decrease. After this the diodes were always kept at temperature below 10°C to avoid reverse annealing. This corresponds approximately to the situation expected in the real ATLAS experiment where full beneficial annealing takes place while the reverse annealing is essentially suppressed [7]. Further details of the diodes and their irradiation are presented in Table 1.

The detailed CCE measurements have been performed for 5 diodes allowing a large enough bias voltage above that of depletion. Two of them were irradiated by pions and three were irradiated by neutrons with fluences covering the whole range of the fluences used. Therefore, these data can be regarded as fully representative.

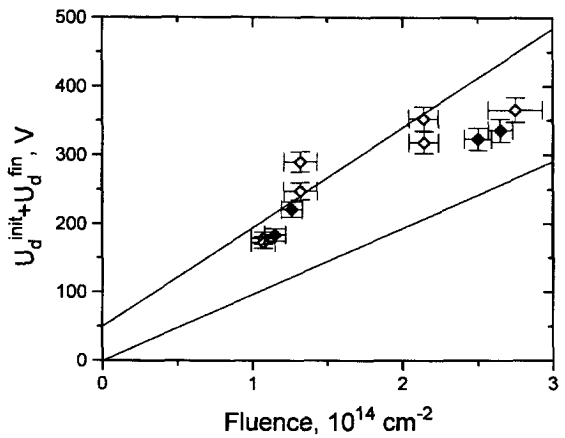

Fig. 1. Change in the depletion voltage (U_d^{fin} + U_d^{init}) corrected to 300 μm diode thickness versus fluence for pion (shaded symbols) and neutron (open symbols) irradiations. The lines show the 1σ area of expected values calculated from the survey of the world data performed in Ref. [7].

2. Depletion voltage

The depletion voltage was measured with the help of an HP-4263A LCR meter. Before irradiation the measurements were performed at room temperature; after irradiation they were performed at 0°C. A frequency of 10 kHz was chosen as a standard for the CV measurements. The value of the depletion voltage was defined by the crossing of the two straight line fits in the log$C$–log$V$ plot. The details of these measurements can be found in Ref. [8]. The error on an individual measurement of the depletion voltage was estimated to be ~ 5%.

As shown in Ref. [8], the depletion voltage measured at 1 kHz is higher by 10–15% than that measured at 10 kHz. This was observed for all temperatures in the range − 16°– + 32°C. This indicates the order of magnitude of systematic effects in this method of determining the depletion voltage.

The change of the depletion voltage versus fluence is presented in Fig. 1. Since type inversion has occurred for all diodes at these fluences [7], the

change in the depletion voltage is the sum of the final and initial depletion voltages: $U_d^{fin} + U_d^{init}$. All the data are corrected to a standard thickness of 300 μm. The lines show the 1σ area calculated from the results of a world data survey performed in Ref. [7]. For this calculation Eq. (4) of Ref. [7] was used taking the parameters from Table 3 of Ref. [7] and neglecting the small exponential term. The reverse annealing contribution was neglected. Practically all the points lie within the expected zone. One can also see that the damage produced by 300 MeV/c pions is very close to that produced by 1 MeV neutrons, in agreement with earlier observations [4].

3. Set up for CCE measurements

Charge collection efficiencies were measured for minimum ionizing particles (MIP) and 5 MeV α-particles with the help of a fast amplifier, BIPOLTEST [9], with a shaping time of ~ 25 ns that matches the front-end electronics to be used for the ATLAS SCT [1]. The very large dynamic range of BIPOLTEST allows the detection of MIPs and α-particles with the same preamplifier. With a diode connected to the amplifier input the noise was < 3000 electrons.

MIP CCE measurements were performed using a collimated ^{90}Sr β-source. A coincidence between two scintillator counters installed one after the other behind the test diode was used as a trigger. This suppressed Bremsstrahlung photon background and allowed selection of β-particles with γ-factor ~ 5, i.e. real MIPs. In measurements with α-particles and ^{57}Co gammas, a trigger from the detector signal itself was used. The preamplifier and scintillator counters are situated inside the refrigerator with an external thermocontrol allowing the temperature of the system to be set at any value between − 25°C and + 20°C with ~ 1°C variations. Further details of the set-up can be found elsewhere [2,10].

A typical MIP spectrum is shown in Fig. 2 together with the corresponding Landau fit. The curve represents a convolution of the Landau function with a Gaussian smearing due to noise and atomic binding effects. The details of the fit may be found in Ref. [2]. The good quality of the trigger is illustrated by the absence of false triggers that should appear as the pedestal peak around channel 13 of the histogram. This also shows that our system has no lower limit in the measurement of CCE values for MIPs.

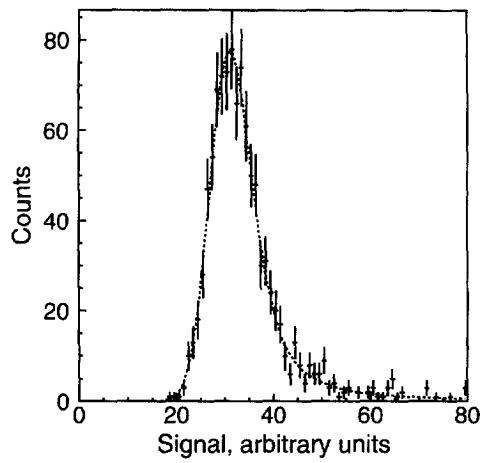

Fig. 2. Typical MIP signal spectrum with Landau fit. The pedestal position is 13.2 histogram bins.

A typical spectrum for α-particles is presented in Fig. 3. The large signal in this case allowed self-triggered CCE measurements down to a few percent level. The peak position was found by a Gaussian fit also shown in the Fig. 3. Gamma quanta from a ^{57}Co radioactive source with 122 keV energy were used for the absolute calibration of the system. A typical ^{57}Co spectrum is shown in Fig. 4. The photopeak position was determined by a Gaussian fit as shown in the histogram.

Before the irradiation all the measurements were performed at room temperature, but after irradiation a temperature of + 10°C or 0°C was used in order to suppress the dark current and to prevent reverse annealing during the measurement period. Note that the operation temperature for the ATLAS SCT is expected to be between 0°C and − 10°C.

4. CCE results

For each diode, the most probable value of the Landau distribution Δ_{mp} was measured before

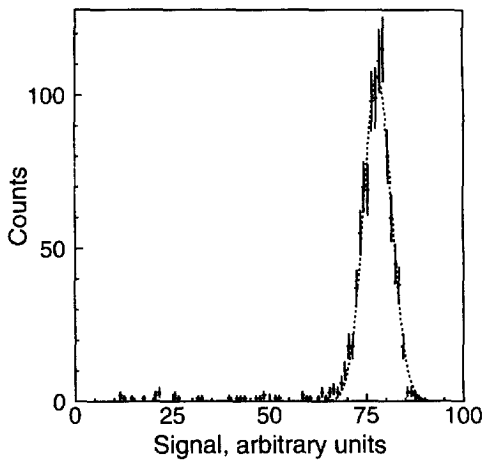

Fig. 3. Typical α-particle signal spectrum with a Gaussian fit.

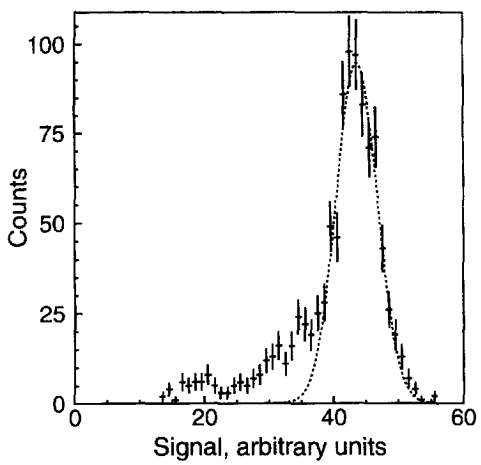

Fig. 4. Typical ^{57}Co signal spectrum with a Gaussian fit of the photopeak. The low energy tail is due to Compton scattering.

irradiation at 100 and 120 V bias. Within $\sim 1\%$ statistical errors the results at these two voltages agree. For a few diodes it was verified that further increase of the voltage also did not change the result. Normalizing Δ_{mp} by the calculated value of $dE/dx = 270\,eV/\mu m$ [2] allowed a measurement of the diode thickness. It was checked that with $\sim 2\%$ accuracy, this thickness agrees with the nominal wafer thickness available for some of the diodes.

The MIP CCE for the irradiated diodes was defined as the ratio between Δ_{mp} observed after irradiation to the value of Δ_{mp} before the irradiation. A complete Landau fit with Gaussian smearing was essential because the visible peak position of the smeared Landau distribution depends on the noise, which was different for the diodes before and after the irradiation due to the large increase of the dark current, especially at the highest voltages used. The maximum voltage was limited either by the hardware limit of 500 V or by the diode breakdown.

The response of the diodes to α-particles for the p^+ and n^+ side illuminations was measured for several diodes before irradiation. The results for different diodes agreed within the $\sim 2\%$ accuracy corresponding to the long term stability of the system, and their average value was used for all the diodes to calculate the α-particle CCE after irradiation. The latter was defined as the ratio of peak position in the α-spectrum to its nominal value for the non-irradiated diode.

A non-irradiated diode with the same geometry as those under study and with depletion voltage of 115 V was used for a direct comparison of the basic features of the charge collection in irradiated and non-irradiated Si detectors. This reference diode was obtained through the CERN RD48 (ROSE) project [11]. The charge collection efficiency for this diode was defined as a ratio of a signal to that on the plateau at high enough bias voltage. The α-particle CCE for this diode are presented in Fig. 5 versus bias voltage. MIP CCE for this diode is shown in Fig. 6 as a function of the normalized depletion thickness $x = (U_{bias}/U_{dep})^{1/2}$. In this plot U_{bias} includes also the "built-in" voltage of 0.5 V. This optimal value for our data includes a possible systematic error in the U_{bias} measurement. The offset in x of the linear extrapolation to CCE = 0 corresponds to $U_{bias} = 0.1$ V. This offset is probably due to a small systematic error in the efficiency measurements at very low bias voltages.

Figs. 7 and 8 show the CCE for the irradiated diodes. The data for the α-particle illumination from the n^+ side are presented in Fig. 7 versus $(U_{bias})^{1/2}$. The CCE for MIPs are presented in Fig. 8 versus bias voltage U_{bias}. The drawing in

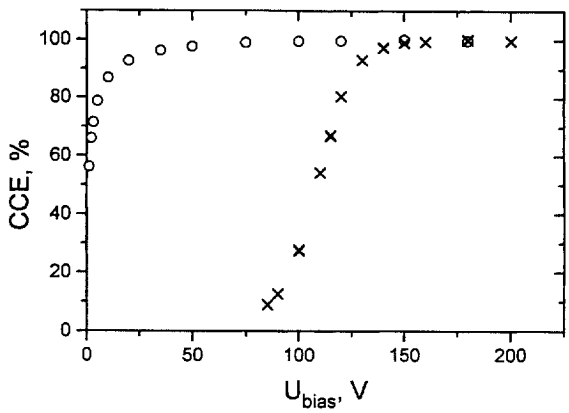

Fig. 5. CCE for α-particle illumination of the p^+(o) and n^+(x) side of the non-irradiated Si detector with $U_{dep} = 115$ V.

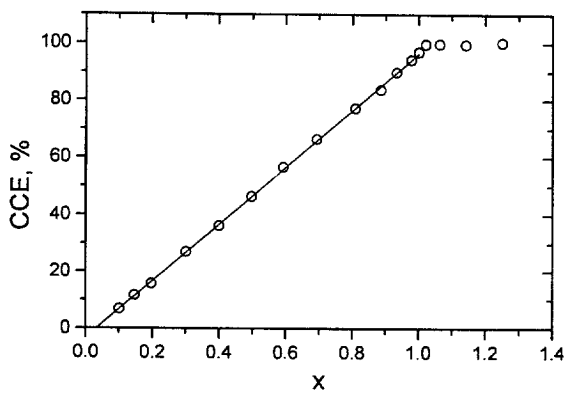

Fig. 6. MIP CCE for the same detector as in Fig. 5 versus normalised depletion thickness $x = (U_{bias}/U_{dep})^{1/2}$. The line is a linear fit through the points with $x < 1$. See text for further details.

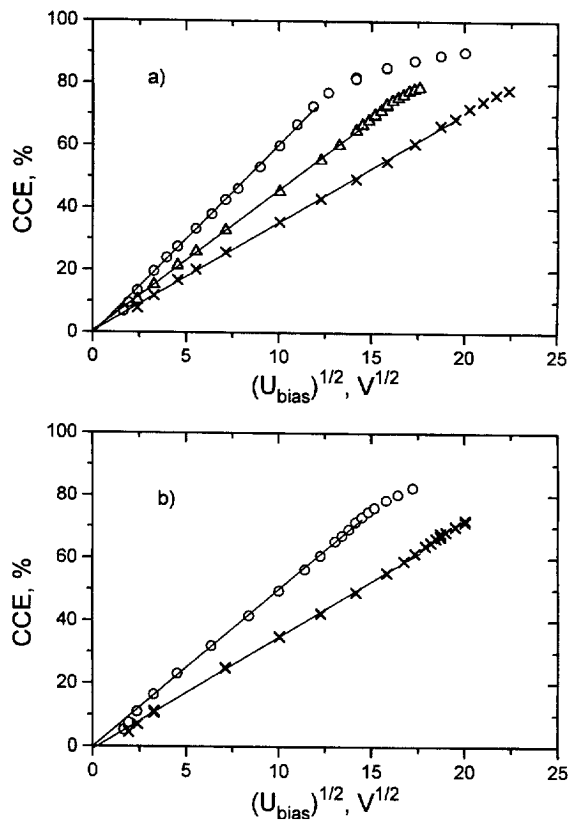

Fig. 7. The CCE for α-particle illumination from the n^+ side versus square root of U_{bias}. The linear fit is made through the points below the depletion voltage. Fig. 7(a) shows the diodes no. 41(circles), 42(triangles) and 46(crosses) irradiated by neutrons, Fig. 7(b) the diodes no. 14(circles) and 28(crosses) irradiated by pions.

Fig. 9 explains the notation used in the discussion that follows.

5. Discussion of the CCE results

In non-irradiated diodes the non-depleted bulk behaves like a metal. Therefore, the α-particle ionization released near the p^+ side should give a 100% signal practically at any voltage. For our reference diode with $U_{dep} = 115$ V even the U_{bias} of 1 V is already sufficient to produce a depletion thickness larger than the α-particles range in Si. The deficit of the p^+ side α-signal for U_{bias} below 50 V that can be seen in Fig. 5 is due to a stretching of the signal current pulse at low U_{bias} so that the integration time of our electronics (70 ns) becomes insufficient for full charge collection (the so-called ballistic deficit). The reason for the current pulse lengthening is the well-known plasma effect [12]. By the same reason the α-particle signal for the n^+ side illumination at the full depletion voltage is considerably lower than 100% and about the same additional bias voltage as for the p^+ side is necessary to suppress the ballistic deficit.

The MIP CCE in the non-irradiated diode presented in Fig. 6 shows a linear behaviour with the

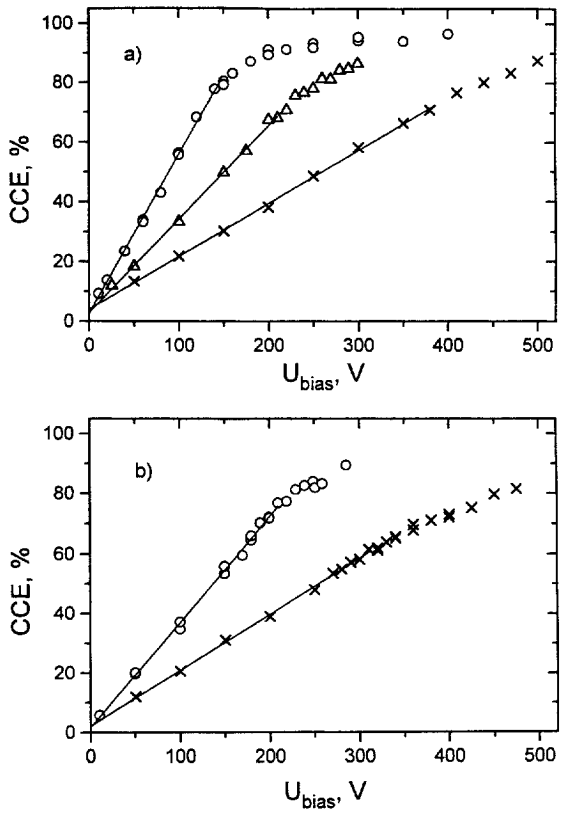

Fig. 8. MIP CCE versus U_{bias} for the same diodes as in Fig. 7. The linear fit is made through the points below the depletion voltage.

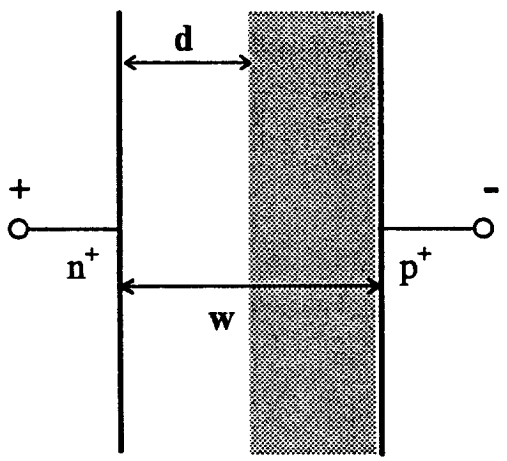

Fig. 9. Schematic diagram of the diode after the type inversion. The non depeleted area of the detector is shaded.

normalised depletion thickness $x = (U_{bias}/U_{dep})^{1/2}$ and saturation for $x > 1$. This is due to the fact that for MIPs the deposited ionization is proportional to the length of the depleted region. The latter grows as a square root of U_{bias} (including the "built-in" voltage). For low density MIP ionisation there is no plasma effect. Therefore, a few volts bias above U_{dep} is sufficient to suppress the ballistic deficit.

The CCE dependencies for the irradiated diodes are radically different from those for the non-irradiated one. For a bias voltage lower than the depletion voltage the α-particle CCE for the n^+ side is proportional to the square root of U_{bias} while the MIP CCE grows linearly with bias voltage as can be seen from Figs. 7 and 8. This can be interpreted as follows.

It has been known for a long time [13] that heavily irradiated Si even in the non-depleted state reacts like an insulator to an AC electrical signal with a period shorter than few microseconds. This is due to the fact that the conductivity in heavily irradiated Si is provided by the deep level defects rather than by shallow level dopants as in the non-irradiated Si. In this sense, heavily irradiated Si is very similar to semi-insulating GaAs. As a result for both of these materials the non-depleted bulk acts as an insulator for a fast electrical signal produced by the drift of electrons and holes released in the active (depleted) part of the detector (for a typical bias value of ~ 200 V and a typical thickness of ~ 300 μm the collection time does not exceed 10 ns). Therefore, the signal development in a detector made of such a material is as follows. The ionization released in the depleted region drifts to the junction electrode and to the edge of the non-depleted (or low electric field) region corresponding to the sign of the carriers. During this drift the signal charge is induced directly on the p^+ and n^+ electrodes of the detector by the carrier electric field penetrating through the non-depleted bulk just as it does through the depleted part of the detector. This fast phase of the collection process ends when the drift of all the carriers released in the active part of the detector is finished (typically in less than 10 ns). After this a slow phase starts during which the carriers stuck near the edge of the non-depleted area are neutralized by the free carriers

arriving from the electrically neutral bulk. As estimated in Ref. [14], the characteristic time for this process in Si is of the order of 400 ns.

For a planar diode and the fast front-end electronics used in our case the above considerations plus Ramo's theorem [15] predict that in a partially depleted detector the signal from the α-particle illumination of the n^+ side will be proportional to the ratio of the active region thickness d to the full detector thickness w. For a uniform space charge this ratio in turn should be equal to $(U_{bias}/U_{dep})^{1/2}$. For MIPs this is also valid, but additionally the amount of the initially released ionization is proportional to the active thickness d. Therefore the MIP CCE should be proportional to $(d/w)^2$ or to the bias voltage U_{bias}.

If carriers are partially trapped during their drift the CCE does not reach 100% even when U_{bias} reaches U_{dep}. The following considerations can explain why this "trapping attenuation" may be almost independent of the bias voltage in a partially depleted detector. In the usual approximation trapping is a function of the ratio of the collection time to the carrier lifetime. Since in an ideal partially depleted detector the drift field goes down to zero at the end of the depleted region the full collection time is meaningless since it diverges logarithmically [2]. Instead a characteristic collection time should be used which can be estimated as the ratio of d to the average drift velocity $\langle v \rangle$. Without saturation $\langle v \rangle$ is proportional to the average drift field U_{bias}/d. Therefore, the characteristic collection time is proportional to d^2/U_{bias} and does not depend on U_{bias}, if the latter is proportional to d^2 as was discussed in the previous paragraph. Together with the collection time the trapping does not change with U_{bias} (if the lifetime itself is not influenced by the bias voltage).

The lines in Figs. 7 and 8 represent the linear fit through the points below depletion and they are drawn up to the depletion voltage only. In the data in Fig. 7 a few points (typically 1–3) at the lowest voltages are not included in the fit since the plasma effect at these voltages induces the ballistic deficit (see above).

For the p^+ side illumination by α-particles a non-zero signal is expected only when the depleted region reaches the p^+ electrode. Surprisingly, a small but clearly detectable signal was observed at much lower voltages. It does not contradict the above hypothesis but requires some electric field also in the non-depleted part of the detector. The analysis of this phenomenon is published elsewhere [16].

When the bias voltage exceeds U_{dep} the collection time decreases with voltage. Thus the attenuation due to trapping can be reduced by a voltage increase as can be seen from Figs. 7 and 8. The CCE data at bias voltages above the depletion voltage for MIPs and α-particle illuminations from both sides allow measurement of the lifetime for electrons and holes separately and a check whether the lifetimes can be considered as independent of the bias voltage. This analysis (complicated by the plasma effect [12] for the α-particle signals) is reported elsewhere [17]. One of the results of this analysis is that in practically all situations the electron and hole contributions to the MIP signal are similar. Therefore, our MIP CCE results for planar diodes can be regarded with reasonable accuracy as valid also for a finely segmented detector with any type of electrodes.

The CCE for MIP and α-particle n^+ side illumination measured at the depletion voltage are presented in Table 2 versus U_{dep} and in Fig. 10 versus fluence. For each diode the MIP and α-particle CCEs are very close. This indicates again the similarity in the hole and electron trapping. Neither CCE decreases very much with fluence because the decrease in carrier lifetimes is partially compensated by the decrease in the effective collection time due to the increase in the applied voltage. In Fig. 11 the MIP CCE at a fixed bias voltage above U_{dep} is shown as a function of fluence for several bias voltages. In this case a rather steep

Table 2
CCE for MIPs and α-particle n^+ side illumination at the depletion voltage

Diode no.	$U_{dep}(V)$	MIP CCE (%)	α-n^+ CCE (%)
41	143	78.4 ± 1.6	73.4 ± 1.5
14	209	76.8 ± 1.5	73.1 ± 1.5
42	211	68.4 ± 1.5	66.8 ± 1.5
28	309	61.2 ± 1.2	62.3 ± 1.3
46	386	71.9 ± 1.4	69.6 ± 1.4

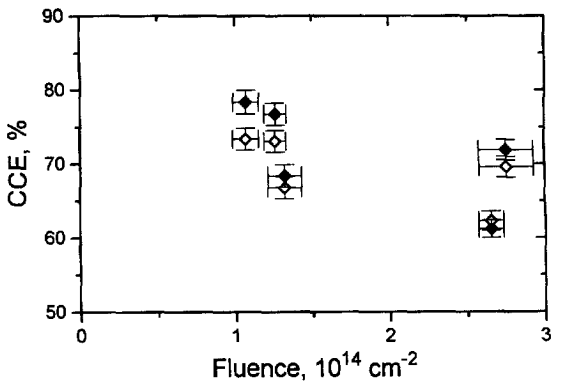

Fig. 10. MIP (shaded symbols) and n^+ side α-particle CCE (open symbols) at the depletion voltage versus fluence.

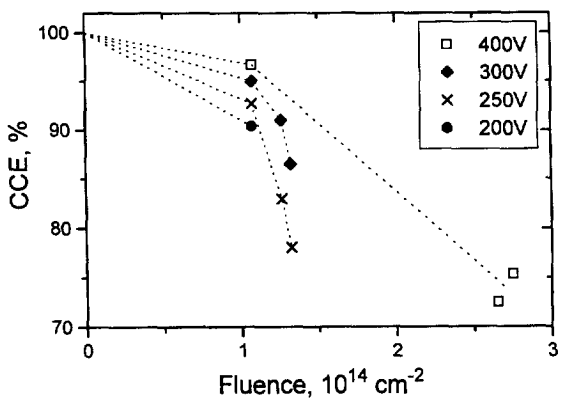

Fig. 11. MIP CCE versus fluence for several fixed bias voltages above the depletion voltage. The lines are drawn to guide the eye.

decrease of the signal with fluence is obvious. The scale of the effect agrees with earlier observations [3,4].

6. Conclusions

The CCE measurements show that after irradiation in a partially depleted planar diode the MIP signal is proportional to the bias voltage while the α-particle signal for the n^+-side illumination is proportional to the $(U_{bias})^{1/2}$. This can be consistently interpreted as a result of the following phenomena:

1. the depleted area grows with voltage from the n^+ electrode (p-type Si);
2. the active (depleted) thickness of the detector grows proportionally to the $(U_{bias})^{1/2}$;
3. non-depleted part of the heavily irradiated Si detector behaves like an insulator for the fast electrical signals produced by the drift of carriers released by an ionizing particle;
4. signal attenuation due to carrier trapping in a partially depleted detector is almost independent of the bias voltage.

For a fluence range $(1–3)10^{14}$ cm^{-2} the MIP CCE at the depletion voltage depends weakly on the fluence, while for any fixed bias voltage above the depletion voltage the CCE decreases with fluence rather steeply.

Acknowledgements

The authors would like to express their gratitude to B.K. Jones and J. Santana for helpful discussions and to S. Holt and D. Campbell for technical support. The help from M. Edwards and D. Hill from RAL in performing the neutron irradiation and from K. Gabathuller (PSI) in performing the irradiation by pions is gratefully acknowledged.

References

[1] CERN LHCC/97-17; ATLAS TDR 5, 30 April 1997.
[2] S. Bates et al., Nucl. Instr. and Meth. A 337 (1993) 57.
[3] F. Lemeilleur et al., Nucl. Instr. and Meth. A 360 (1995) 438.
[4] S.J. Bates et al., Nucl. Instr. and Meth. A 379 (1996) 116.
[5] J.D. Richardson, Ph.D. Thesis, University of Liverpool, 1995.
[6] T. Angelescu, A. Vasilescu, Nucl. Instr. and Meth. A 374 (1996) 85.
[7] A. Chilingarov et al., Nucl. Instr. and Meth. A 360 (1995) 432.
[8] L. Beattie et al., ROSE (RD-48) Technical Note 97/4, March 1997.
[9] P. Jarron et al., in: L. Cifarelli, T. Ypsilantis (Eds.), New Technologies for Supercolliders, Plenum Press, New York, 1991, pp. 105–123.
[10] A. Chilingarov, T. Sloan, Proc. 3rd Int. Workshop on Gallium Arsenide and Related compounds, San Miniato, Italy, March 21–24 1995, World Scientific, Singapore, p. 52.

[11] RD48 Status Report, CERN/LHCC 97-39, 20 June 1997.
[12] R.N. Williams, E.M. Lawson, Nucl. Instr. and Meth. 120 (1974) 261.
[13] Z. Li, H.W. Kraner, IEEE Trans. Nucl. Sci. NS-38 (1991) 244.
[14] G. Lutz, Nucl. Instr. and Meth. A 377 (1996) 234.
[15] S. Ramo, IRE 27 (1939) 584.
[16] L. Beattie et al., The electric field in irradiated silicon detectors, ATLAS Internal Note INDET-No-194 (1997) Nucl. Instr. and Meth. A, To be submitted.
[17] T.J. Brodbeck et al., Carrier lifetimes in heavily irradiated Si diodes, Nucl. Instr. and Meth. A, To be submitted.